
	Ref	CCI Biomass Product Validation Plan v3		
	Issue	Page	Date	
	1.0	1	25-01-2021	



CCI BIOMASS

PRODUCT VALIDATION PLAN YEAR 3 VERSION 3.0

DOCUMENT REF:	CCI_BIOMASS_PVP_V1
DELIVERABLE REF:	D2.5-PVP
VERSION:	3.0
CREATION DATE:	14-01-2021
LAST MODIFIED	25-01-2021

Document Authorship

	NAME	FUNCTION	ORGANISATION	SIGNATURE	DATE
PREPARED	Sytze de Bruin	WP7000	Wageningen University		
PREPARED	Martin Herold	WP7000	Wageningen University		
PREPARED	Arnán Araza	WP7000	Wageningen University		

	Ref	CCI Biomass Product Validation Plan v3		
	Issue	Page	Date	
	1.0	2	25-01-2021	

PREPARED	Richard Lucas	Project Manager	Aberystwyth University		
PREPARED					
PREPARED					
PREPARED					
PREPARED					
PREPARED					
PREPARED					
VERIFIED	S. Quegan	Science Leader	Sheffield University		
APPROVED					

Document Distribution



ORGANISATION	NAME	QUANTITY
ESA	Frank Seifert	

Document History

VERSION	DATE	DESCRIPTION	APPROVED
0.1	14-01-2021	First draft version	
1.0	25-01-2021	Revised version	



Document Change Record (from Year 1 to Year 2)

VERSION	DATE	DESCRIPTION	APPROVED

	Ref	CCI Biomass Product Validation Plan v3		
	Issue	Page	Date	
	1.0	3	25-01-2021	



CONTENTS

List of tables.....	4
List of figures	5
Symbols and acronyms.....	6
1. Introduction	7
2. Concepts	9
2.1. Definitions.....	9
2.2. Statistics.....	9
3. Database compilation	11
3.1. Sources of reference data	11
3.2. Sampling design	11
3.3. Tiers of plot data and other in situ data.....	12
3.4. Data harmonization.....	14
4. Map-plot comparisons	16
4.1. Assumptions	16
4.2. Descriptive analyses	16
4.3. Stratification and spatial aggregation	17
4.3.1. Comparisons at 0.1° cell resolution	17
4.3.2. Ecoregions	18
5. Spatial uncertainty modelling.....	19
5.1. Definition of the error model	19
5.2. Identification of the error model	20
5.2.1. Overview.....	20
5.2.2. Variograms of AGB from small plots.....	20
5.2.3. Variograms of map error at the spatial support of map pixels.....	21
5.3. Model-based prediction	21
5.3.1. Bias trend prediction	21
5.3.2. Error budgeting.....	21
5.3.3. Block kriging for map-plot comparison at supra pixel support.....	22
5.3.4. Spatial aggregation of random error	22
6. Map inter-comparison.....	23
6.1. Stability of $AGB_{map} - AGB_{ref}$ among CCI Biomass products	23
6.2. Comparison of CCI Biomass maps with other AGB products.....	24
7. Expert assessment.....	25
References	27
APPENDIX 1.....	29

	Ref	CCI Biomass Product Validation Plan v3		
	Issue	Page	Date	
	1.0	4	25-01-2021	



LIST OF TABLES

Table 1. Statistics used in this PVP.	10
Table 2. Estimation methods for the parameters of the uncertainty model.	20

	Ref	CCI Biomass Product Validation Plan v3		
	Issue	Page	Date	
	1.0	5	25-01-2021	



LIST OF FIGURES

Figure 1. Validation objectives (left) and derived validation activities (right).	7
Figure 2. Geographical locations of plots and footprints (CoFor and LiDAR) of the reference datasets collected up to January 2021.	13
Figure 3. Overview of data harmonization steps.	15
Figure 4. Example of a $AGB_{map} - AGB_{ref}$ comparison plot taken from de Bruin et al. (2020b).	16
Figure 5. AGB residuals between harmonized tier1-3 plot data and mapped AGB at 0.1° cell level for each combination of map reference years. The red dashed line is the 1:1 line.	23
Figure 6. Example comparison of different global biomass maps (Baccini, GOCARBON and GlobBiomass) against harmonized plot data.	24
Figure 7. Screenshot of a prototype analysis tool provided with the R package for expert assessment.	25

	Ref	CCI Biomass Product Validation Plan v3		
	Issue	Page	Date	
	1.0	6	25-01-2021	

SYMBOLS AND ACRONYMS

AGB	Above ground biomass density (in general)
AGB _{map}	Aboveground biomass density according to the map
AGB _{plot}	In situ aboveground biomass density
AGB _{ref}	AGB _{plot} , corrected for inventory date and if footprint < 1 ha corrected for forest fraction
AGB*	True above ground biomass density
ALS	Aerial Laser Scanning
CCI	Climate Change Initiative
CCI-Biomass	Climate Change Initiative – Biomass
CEOS	Committee on Earth Observation Satellites
CI	Confidence Interval
CoFor	Congo basin Forests AGB dataset (Ploton et al., 2020)
DARD	Data Access Requirements Document
ECV	Essential Climate Variables
ESA	European Space Agency
IPCC	Intergovernmental Panel on Climate Change
LIDAR	Light Detection And Ranging
LPV	Land Product Validation
MSE	Mean Squared Error
NEON	National Ecological Observatory Network, USA
PI	Prediction Interval
PVP	Product Validation Plan
RMSE	Root Mean Squared Error
SAR	Synthetic Aperture Radar
SD	Standard Deviation
SLB	Sustainable Landscape Brazil
TERN	Terrestrial Ecosystem Research Network, Australia
Var	Variance
$\gamma_{AGB}(h)$	Variogram model of AGB with a spatial support matching the smallest plot size used our analyses
$\gamma_M(h)$	Variogram model of the residuals between AGB _{map} and AGB _{ref} , with a spatial support matching the map pixels.

	Ref	CCI Biomass Product Validation Plan v3		
	Issue	Page	Date	
	1.0	7	25-01-2021	

1. Introduction

This consolidated version of the Validation Plan aims to provide a common framework for assessing and reporting the accuracy of the CCI Biomass products, namely the 2010, 2017 and 2018 global biomass maps as well as the corresponding uncertainty layers, and to assess user appreciation of these products. Elaboration of the plan and the forthcoming validation itself run in parallel with ongoing Committee on Earth Observation Satellites (CEOS) cal/val development, which provides opportunities for co-creation of the CEOS cal/val procedure. We further build on the results of the GlobBiomass project (Avitabile et al. 2015, Rozendaal et al. 2017).

The framework consists of five main activities that jointly lead to the achievement of the validation objectives, as shown in Figure 1.

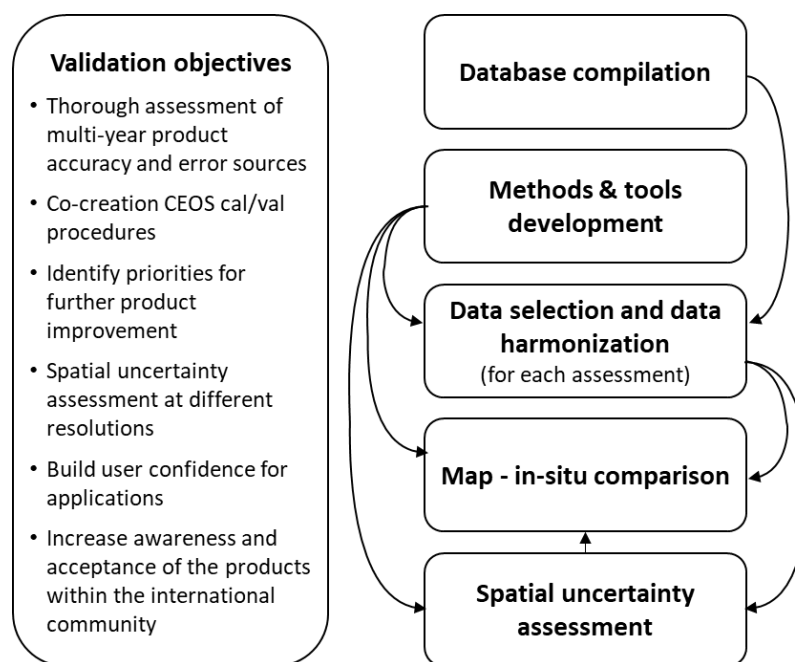




Figure 1. Validation objectives (left) and derived validation activities (right).

As with its predecessors (de Bruin et al. 2019a, de Bruin et al. 2020a), this Product Validation Plan (PVP) is developed in line with the current draft of the new CEOS Land Product Validation (LPV) protocol for biomass from space calibration and validation. The new CEOS protocol contains a dedicated section about using existing in situ data as reference for the validation of larger area biomass maps, assuming they are properly screened, processed and harmonized. It is recognized that different users including national inventory experts, global climate modelers and local project implementers all have specific needs when it comes to biomass estimation and uncertainty assessment with respect to spatial resolution, geographic extent, timing, thematic content and definitions, and type and standards of uncertainty reporting. The CCI Biomass project and its climate users are also interested in spatially explicit assessments of map precision and map bias in addition to the more standard accuracy analysis undertaken for biomass map validation exercises.

This requires an effort to include a large number of in situ data sources covering all major geographical regions and forest types (top box on the right of Figure 1). The main data sources of forest biomass information include National Forest Inventories (NFIs), research forest plot networks and operational

	Ref	CCI Biomass Product Validation Plan v3		
	Issue	Page	Date	
	1.0	8	25-01-2021	

monitoring stations established for forestry, ecology or environmental purposes, including those that use local LIDAR observations to provide biomass reference data.

The second box from the top at the right-hand side of Figure 1 indicates that a common set of data harmonization and analysis methods and tools is developed and used. To support wider use, these are provided in the form of an R-package that allows the climate change community (both within and outside the project) to assess biomass maps based on their own reference data, without the need to upload those data to an external database.



The centre box at the right-hand side of Figure 1 refers to in situ data selection from the database, based on a set of quality criteria. The box further denotes data harmonization to adjust for partial forest cover of map pixels and allowable (< 10 years) temporal mismatches between the map reference year and the in situ AGB inventory date.

Map-plot comparison (fourth box from the top in Figure 1) concerns statistical assessment of differences between map and in situ above ground biomass (AGB) over reference AGB ranges. The assessments are performed at the map pixel level, as well as spatially aggregated over larger pixel blocks. They are also differentiated over ecoregions, realms¹ and slope and aspect classes which have been found to affect AGB retrieval from satellite data (e.g., Réjou-Méchain et al. 2019). The aims of the map-plot comparisons are to assess whether the biomass map satisfies design specifications (relative error of less than 20% where AGB exceeds 50 Mg ha⁻¹) and provide map producers with information on how and where to improve their products. It is important to realize that the reference data are also estimates and therefore affected by errors that should be taken into account when using them in the map-plot comparisons (Réjou-Méchain et al. 2017, Réjou-Méchain et al. 2019). This is indicated by the short upward arrow in the bottom-right of Figure 1.

During the CCI Biomass User Workshops and later communications, the climate, carbon cycle and REDD+ communities expressed the need for unbiased biomass estimates accompanied by spatially explicit uncertainty information at spatial resolutions ranging from the 1 ha resolution of CCI Biomass up to 0.5 or even 1-degree cells (for climate modelling) or countries (for REDD+) (Quegan and Ciais 2018). Hence, CCI Biomass product validation should explicitly address estimation of systematic deviations and random differences between reference and map biomass and uncertainty assessment at different spatial aggregation levels. This is indicated by the box at the bottom-right of Figure 1.

Details on the approaches are provided in later chapters of this validation plan.

¹ Biogeographic realms are large spatial regions within which ecosystems share a broadly similar biological evolutionary history. Eight terrestrial biogeographic realms are typically recognized, corresponding roughly to continents. See Dinerstein, et al. (2017).

	Ref	CCI Biomass Product Validation Plan v3		
	Issue	Page	Date	
	1.0	9	25-01-2021	

2. Concepts

2.1. Definitions

Accuracy is only occasionally used in this document to *qualitatively* refer to both random and systematic error. This use of the term is in line with the ISO 5725 definition of accuracy.

Bias expresses the degree to which the expected value of an estimator differs from the true underlying quantitative parameter being estimated.

Error. For a continuous variable such as AGB, error is defined as the difference between our representation of reality (e.g., a mapped AGB value) and reality (e.g., a true AGB value). We can only know error at some locations, if at all, because we rely on scarce reference values (e.g., from plots) which themselves are estimates of reality. Therefore, we will often refer to **differences** or **residuals** between mapped AGB values and reference AGB.

Precision denotes the dispersion of random errors; it is expressed by measures of statistical variability such as variance and standard deviation.

Stability. According to the World Meteorological Organization (2011), stability is the extent to which the error of a product remains constant over a long period longer period of time.

Systematic deviation of biomass refers to a systematic difference between predicted biomass (on the map) and reference biomass obtained from plot data. Only if plot data (which themselves are estimates) are unbiased, systematic deviation would equal bias. We assume plot data to be unbiased.

Uncertainty is a *quantitative* acknowledgement of error: we are aware that our representation differs from reality, but we are only able to model the distribution of error (expressed by a probability distribution), rather than the error itself. This is a common situation, because if we knew error, we would simply correct for it and reduce the error to zero.

2.2. Statistics

Table 1 lists the statistics used in this PVP, as well as their definitions, where E is the expected value, Z denotes a random variable, μ is the mean of Z , Y is a vector of n reference values, \hat{Y} is a vector of n predicted values (i.e., CCI-Biomass predictions), and h denotes a distance between two locations x .





	Ref	CCI Biomass Product Validation Plan v3		
	Issue	Page	Date	
	1.0	10	25-01-2021	

Table 1. Statistics used in this PVP.

Acron.	Name	Description	Definition
Var	Variance	Measure of spread of a random variable (Z)	$Var(Z) = E[(Z - \mu)^2]$
SD	Standard deviation	Measure of spread of a random variable; square root of the variance	$SD(Z) = \sqrt{Var(Z)}$
d_i	Observed difference	Difference between a predicted value, \hat{y}_i and a reference value, y_i , where i refers to a particular instance, e.g., a location.	$d_i = \hat{y}_i - y_i$
MD	Mean difference	Average difference between reference values and predicted values	$MD = \frac{1}{n} \sum_{i=1}^n d_i$
MSD	Mean squared difference	Average squared difference between reference values and predicted values	$MSD = \frac{1}{n} \sum_{i=1}^n d_i^2$
RMSD	Root mean squared difference	Square root of MSD	$RMSD = \sqrt{MSD}$
CI	Confidence interval	Measure of uncertainty associated with a sample population estimate (e.g., μ); intervals covering individual observations commonly referred to as prediction intervals (see below).	Estimated range of values likely to include an unknown population property.
PI	Prediction interval	Measure of uncertainty associated with the prediction of single observations	Estimated range in which a new observation falls, with a certain probability, given an existing model
$\gamma(h)$	(Semi)variogram	Function describing the degree of spatial dependence of a spatial random field, where x is a spatial position and h is a distance lag	$\gamma(h) = \frac{1}{2} Var[Z(x) - Z(x+h)]$
$\sigma_{i,j}$	Spatial covariance	Element of the spatial covariance matrix, Σ , where i and j ($1 \dots n$) refer to pixels within a spatial unit	$\sigma_{i,j} = E[Z(x) - E(Z(x))] \cdot E[Z(x+h) - E(Z(x+h))]$

	Ref	CCI Biomass Product Validation Plan v3		
	Issue	Page	Date	
	1.0	11	25-01-2021	

3. Database compilation

3.1. Sources of reference data

Building upon the GlobBiomass reference database (Rozendaal et al. 2017), an extensive dataset of forest in situ data across the world has been acquired for the purpose of the validation (see Appendix 1, Figure 2 and also the DARD (Lucas, et al., 2020)). Plots included in the database undergo a series of quality checks (see below). In situ forest data were not used for calibration of the CCI Biomass map to guarantee full independence from the production process and because the project's biomass map processing chain does not rely on such calibration procedure.

The following in situ data selection criteria are used for CCI Biomass product validation. In situ data need:



- A proper citable reference source and metadata to assess the procedures and quality of biomass estimation.
- Precise coordinates (4-6 decimals for coordinates in decimal degrees).
- A census date within ten years from the reference year of the AGB map to avoid temporal inconsistency with the assessed maps.
- Measurements of all trees of diameter ≥ 10 cm (or less) are included in the estimates.
- Sites that were not deforested between the year of the inventory and the reference year of the CCI Biomass map (i.e., 2010, 2017 and 2018). The latter assessment is based on the 2018 forest loss layer of the Hansen dataset (Hansen et al., 2013).
- LiDAR-derived AGB or other indirect AGB data, with these accompanied by estimates of the standard deviation of AGB error.

Note that the current data agreements will have to be renewed and new agreements will have to be established.

3.2. Sampling design

We rely on AGB in situ data that are not specifically produced for validation purposes but that are rather collected within the context of national forest inventories and other efforts at local to regional scale. This has several consequences, which are summarised as follows:

- The populations of the CCI Biomass products and those of the inventories differ. CCI Biomass concerns forest biomass over the entire globe (including areas without forest), whereas forest inventories typically only concern forested areas within countries or regions. Moreover, large portions of the world including Southeast Asia, large parts of Africa, the dry tropics and Siberia have very little or no in situ data at all (see Figure 2).
- The sampling frames are different: CCI Biomass concerns mean forest biomass density discretised in $\sim 100\text{m} \times 100\text{m}$ pixels (including non-forested area) while the inventories employ non-uniformly sized and typically small plots (on average 0.15 ha for the AGB plot data referred to in Appendix 1) within forested areas.

	Ref	CCI Biomass Product Validation Plan v3		
	Issue	Page	Date	
	1.0	12	25-01-2021	

- Regionally, the AGB plot locations may have been chosen by probability sampling but large areas of the world are not included in the AGB plot sample (see first bullet). That is because in these areas there are no forest inventories or because institutions or authorities are unwilling to share inventory data.
- The wide variety of sampling designs included in the AGB in situ dataset produces a complex amalgamated sample.

Given the above, our approach is to consider the AGB in situ data with its mix of plot sizes or footprints and local sampling designs as an opportunistic sample (also referred to as an ad hoc sample by other authors). Such sampling invalidates conventional statistical inference methods unless particular assumptions are made (see section 4.1).

Additionally, a model-based approach is adopted here, with the model parameters estimated from the in situ data along with other data sources (see section 5.2). Absence of in situ data in large portions of the world forces us to apply model parameters (trend models of systematic deviation and correlograms) estimated for ecological zones or continents in areas where they cannot be verified but which are assumed to have similar characteristics.

3.3. Tiers of plot data and other in situ data

The contributions of AGB measurement error and within-pixel sampling error (see section 5.1) are known to be largest for small plots such as National Forest Inventory (NFI) plots, while detailed measurements of all trees within large plots are deemed to deliver highest quality AGB data (Réjou-Méchain et al. 2014, Réjou-Méchain et al. 2019).

A straightforward approach for taking into account expected differences in the accuracy of plot data is to adopt a tiered approach comprising (tier 1) small plots (≤ 0.6 ha) including National Forest Inventory (NFI) data, (tier 2) larger plots with sizes in the range 0.9-3 ha, and (tier 3) high-quality large super-plots (≥ 6 ha; such as from Labrière et al. (2018)).

In addition to the above tiered plot data, we use LiDAR-based AGB data at 100 m resolution from the Sustainable Landscape Brazil project (SLB), the National Ecological Observatory Network, USA (NEON) and the Terrestrial Ecosystem Research Network, Australia (TERN) processed by Labrière and Chave (2020a, b, c). Yet another data source concerns 1-km pixel forest management inventory data originating from the Congo basin Forests AGB (CoFor) dataset (Ploton et al., 2020). Concerning the latter dataset, only pixels having at least five in situ forest management inventoried plots are proposed to be used.

These tiered plot data, the LiDAR and the CoFor data are analysed separately in the descriptive plot-pixel comparisons (section 4.2).

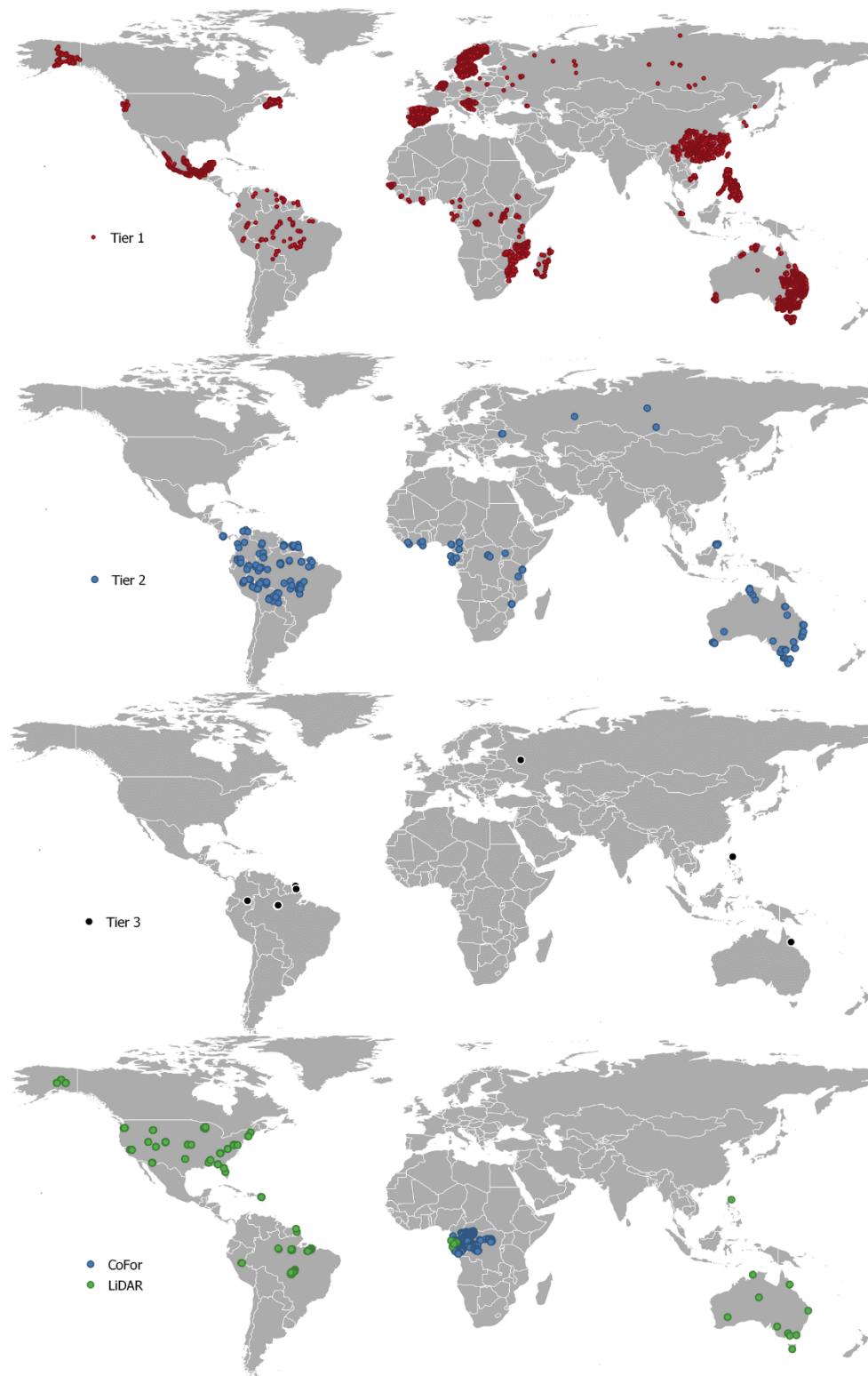




Figure 2. Geographical locations of plots and footprints (CoFor and LiDAR) of the reference datasets collected up to January 2021.

	Ref	CCI Biomass Product Validation Plan v3		
	Issue	Page	Date	
	1.0	14	25-01-2021	

3.4. Data harmonization

For AGB product validation, the response design encompasses all steps leading to the assessment of differences between map and plot AGB (cf. (Olofsson et al. 2014). The plots used in our comparison may have been surveyed at a different time than the map to be assessed, they typically differ in spatial support (i.e., the area covered by individual plots) from the AGB map (AGB_{map}) pixels and they measure different spatial entities (average biomass over a pixel area versus forest biomass within a forest plot). Therefore, data harmonization is needed prior to the analysis of differences.

Differences between the inventory date of AGB plots and the reference year of the AGB map are harmonized using updated IPCC growth rates (IPCC 2019, Requena Suarez et al. 2019) following the approach described in Version 1 of the PVP (de Bruin et al. 2019a). For plots in tropical and subtropical ecological zones, age category dependent growth rates are available (IPCC 2019, Requena Suarez et al. 2019). In those cases, plot AGB values in the range 0-99 Mg/ha are assumed to represent young secondary forest. AGB values in the range 100-152 Mg/ha are treated as old secondary forest (Van Breugel et al. 2007), AGB above 153 Mg/ha is assumed to correspond to old growth stands (Brown et al. 1989, Clark and Clark 2000, Mello et al. 2016). Given the absence of data on plot forest age, mature forests with low AGB cannot be distinguished from young stands, which has potential implications for the applied growth rates. For temperate oceanic forests in Europe and boreal coniferous forests and tundra woodlands, no differentiation of growth rates over age categories is used. The temporal adjustments by growth rates are applied up to a difference of ten years between the inventory date and the map reference year. Plots having a larger temporal difference are discarded in the analyses (see section 3.1). The growth rate table in IPCC (2019) also reports different types of uncertainty estimates, such as confidence intervals (CI). The latter are translated into variances assuming a normal distribution.

Recall that the AGB plot data and the map have distinct sampling populations (see section 3.2) in terms of both different spatial support and the inclusion of non-forested areas within map pixels. Harmonization of these differences is attempted by multiplying the temporally adjusted plot AGB by forest fraction. This forest fraction is computed by putting a 10% threshold on a tree cover product (Hansen et al. 2013) corresponding to the CCI Biomass map reference year. This is undertaken both at pixel level and over larger aggregated blocks. In the rare case of more than one AGB plot occurring within a pixel, the average of the adjusted AGB per plot is used. The correction for forest fraction is applied only to plots with an area below 1 ha.

The data harmonization procedure is pictured in Figure 3. The reference AGB obtained (either at pixel level or over aggregated pixel blocks) is referred to as AGB_{ref} .

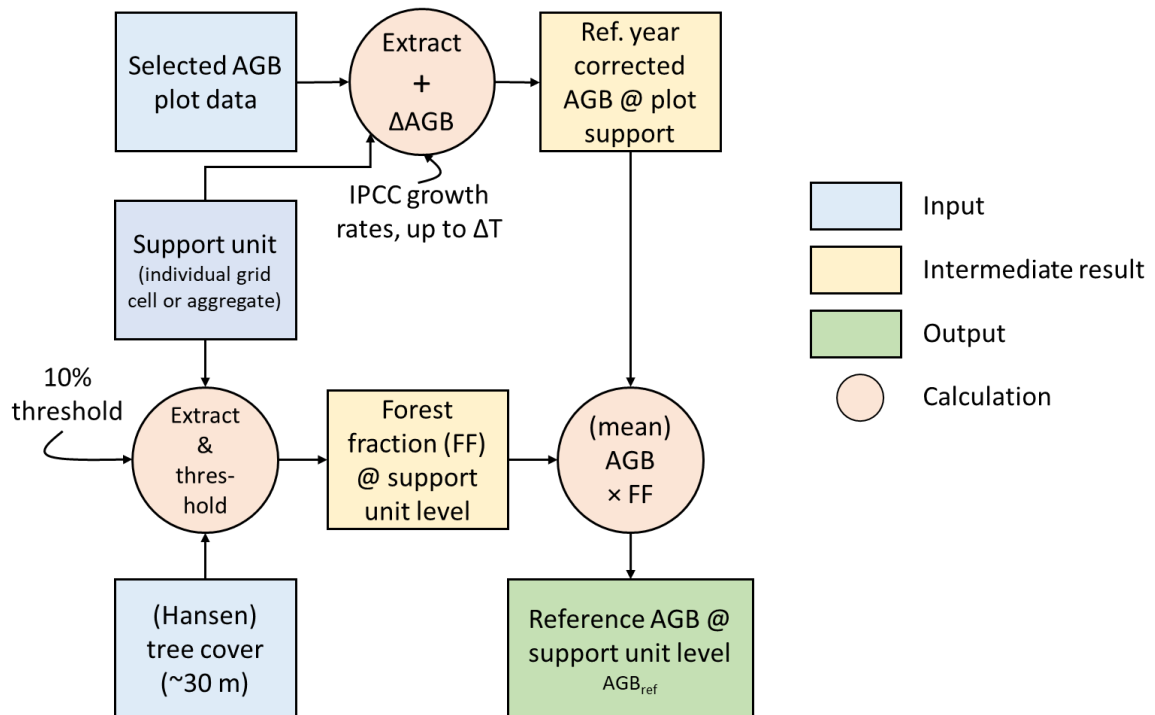




Figure 3. Overview of data harmonization steps.

	Ref	CCI Biomass Product Validation Plan v3		
	Issue	Page	Date	
	1.0	16	25-01-2021	

4. Map-plot comparisons

4.1. Assumptions

After adjustments for temporal discrepancies and partial forest fraction and having at least ten in situ sites within a reference biomass range, we assume mean AGB_{ref} computed from the reference data in tiers 1 and 2 to be unbiased. For tier 3 data (section 3.3), we relax the requirement of 10 plots per biomass range because these data were recorded over large footprints (≥ 6 ha) and the measurements followed a strict protocol.

When reporting mean differences, $AGB_{map} - AGB_{ref}$, and root mean squared difference (RMSD) over spatial strata (see section 4.3) we assume that comparisons of map and in situ data within strata are representative of those strata. For the descriptive analyses (section 4.2) it is further assumed that map-plot comparisons are mutually independent but, in the proposed geostatistical approaches (chapter 5), this assumption is relaxed.

4.2. Descriptive analyses

For tabulation, 50 Mg/ha wide AGB_{ref} bins are used up to 400 Mg/ha, while AGB_{ref} values above 400 Mg/ha are grouped in a single bin, i.e., 0-50, 50-100 ... 350-400 and > 400 Mg/ha. For each bin, the tables list at least the mean AGB_{ref} , mean AGB_{map} , mean $AGB_{map} - AGB_{ref}$ (MD), and the RMSD between AGB_{ref} and AGB_{map} .

For plotting, 25 Mg/ha wide bins are used up to 350 Mg/ha along with a single bin for all higher AGB_{ref} values. The plots have AGB_{ref} on the x-axis and AGB_{map} on the y-axis. Mean (AGB_{ref} , AGB_{map}) pairs are shown using a point symbol while the interquartile ranges of AGB_{map} per bin are depicted by whiskers. An example is shown in Figure 4.

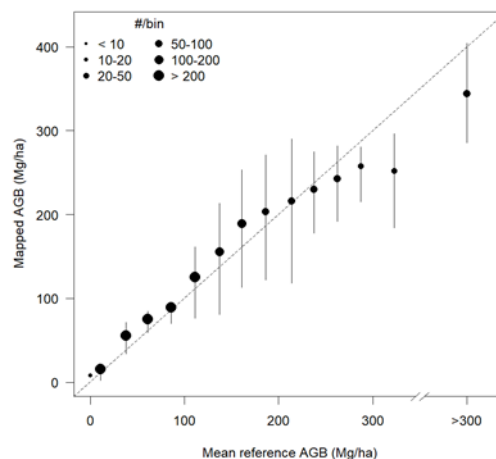




Figure 4. Example of a $AGB_{map} - AGB_{ref}$ comparison plot taken from de Bruin et al. (2020b).

A straightforward way of analysing $AGB_{map} - AGB_{ref}$ differences was anticipated in section 3.3. To account for the expected differences in the accuracy of plots in different size categories, plots in different tiers can be analysed separately. Under the above unbiasedness assumption (section 4.1), mean differences between harmonized in situ data and map values aggregated over bins covering ranges of reference

	Ref	CCI Biomass Product Validation Plan v3		
	Issue	Page	Date	
	1.0	17	25-01-2021	

AGB values are interpreted as map bias, per tier. However, note that binning of in situ data affected by random errors may falsely suggest map bias. This has been demonstrated for the within-pixel sampling error in the latest PVIR (de Bruin et al., 2020b, Figures 17 and 18). To empirically verify the assumption of unbiased in situ data, the analyses are conducted for each of the tiers other data sources and consistency of results is assessed whenever data volume allows this.

An alternative to the tiered approach is to weight $AGB_{map} - AGB_{ref}$ differences within bins using inverse variance weighting based on the sum of the in situ measurement error variance, the variance of the error introduced at the data harmonization steps (section 4.2.1), and the plot-pixel sampling error. These error variances are explained in section 5.1. Such an approach is only possible if sufficient data are available for assessing spatial correlation structures of the latter error component for the smallest footprint size.

In case weighted (AGB_{ref} , AGB_{map}) pairs are computed, weighted quantiles and RMSD are also used for tabulation and plotting.

4.3. Stratification and spatial aggregation

4.3.1. Comparisons at 0.1° cell resolution



Depending on how data are used, biomass map users (e.g., climate modellers and REDD+ communities) may be interested in uncertainties over larger support units, such as square pixel blocks (Quegan and Ciais 2018). Aggregation of biomass predictions and measurements over larger spatial units often results in a partial cancelling out of *random* prediction errors and measurement errors. Note that this does not hold for systematic error or bias. Therefore, aggregation is expected to improve the precision of map and harmonized plot data if both map and multi-plot data are averaged over larger spatial units.

To assess the CCI Biomass map at a resolution commonly used by climate modellers, $AGB_{map} - AGB_{ref}$ comparisons are also made over multi-pixel blocks at the 0.1° cell resolution. In this case, correction for partial forest fraction (see above) is undertaken at the level of the coarse resolution cells. Mean AGB_{ref} at 0.1° cell resolution is computed by multiplying forest fraction at the 0.1° cell level with the mean temporally adjusted AGB plots in that cell (see Figure 3).

Three options are considered for calculating the latter mean temporally adjusted AGB at the 0.1° cell level.

- Using unweighted means for each of the tiers and other data sources (LiDAR/CoFoR) separately (cf. section 4.2).
- Inverse variance weighting of in situ data based on the sum of the AGB measurement error variance, the variance of the error introduced at the data harmonization steps (section 3.4), and the within-pixel sampling error. This option still assumes mutual independence of plot data but explicitly accounts for different quality plot data.
- Relaxing the mutual independence of in situ data, another option is to compute block averages by a block kriging approach (Goovaerts 1999, Malone et al. 2013).



Our aim is to compare the above options but the latter two are only feasible if sufficient data are available for assessing spatial correlation structures (variograms $\gamma_{AGB}(h)$) of AGB for the smallest plot

	Ref	CCI Biomass Product Validation Plan v3		
	Issue	Page	Date	
	1.0	18	25-01-2021	

size used in the analyses. The thus obtained AGB reference values are compared with the average AGB_{map} over the corresponding 0.1° cells.

4.3.2. Ecoregions

$AGB_{map} - AGB_{ref}$ comparisons at 0.1° cell resolution (see above) are also stratified according to ecoregions derived from the recent global ecoregion map (Dinerstein et al. 2017), which can be downloaded from <https://ecoregions2017.appspot.com/>. To this end, the original vector maps are rasterized to 0.1° resolution. Resulting raster cells are assigned to the category covering the largest portion of the cell area.

	Ref	CCI Biomass Product Validation Plan v3		
	Issue	Page	Date	
	1.0	19	25-01-2021	

5. Spatial uncertainty modelling

5.1. Definition of the error model

Even though the in situ AGB data are assumed unbiased, they are not error-free and therefore comparisons between AGB maps and AGB in situ data should be accompanied by an uncertainty analysis. The first step in such analysis is definition of the error model. We propose an additive model expressing the difference between a map prediction AGB_{map} and reference AGB_{ref} at pixel x (denoted as $D(x)$) as a random variable composed of five *zero mean* random error components and a map bias component (Equation 1):

$$D(x) = M(x) - (Plt(x) + Pos(x) + H(x)) + S(x) + b(x) \quad (1)$$



where $M(x)$ the map biomass error at location x , $Plt(x)$ is the plot measurement error (Réjou-Méchain et al. 2017), $Pos(x)$ is a positional error component, $H(x)$ is the error introduced at the data harmonization steps (section 3.4), $S(x)$ is a within-pixel sampling error component, and $b(x)$ is the map bias, i.e., the difference $AGB_{map}(x) - AGB^*(x)$, where the latter term is the true biomass density for pixel x . The within-pixel sampling error, $S(x)$, arises because the AGB plot size is usually small compared to the ~ 1 ha AGB map pixel (see Appendix 1). It is defined as $AGB^*(x) - AGB^*_{plot}(x)$, where the latter term is the true biomass at the spatial support of in situ data within the pixel. A pixel footprint covered by a homogeneous forest biomass population has sub-pixel biomass variation, and the plot samples only part of that. Pixel footprints partly covered with forest undergo a harmonization procedure as explained in section 3.4. Note that $S(x)$, $Plt(x)$, $Pos(x)$, $S(x)$ and $H(x)$ are random variables whose values are unknown but can be described by probability distributions (Heuvelink, 2005).

All random error terms at the right-hand side of Equation (1) (i.e., all terms except $b(x)$) are assumed to be zero mean and mutually uncorrelated. If the plot has small size relative to the pixel, $Pos(x)$ is not relevant unless the plot is at the edge of the pixel; all that matters is that it is located within the pixel. Earlier analyses using a conservative distance decay function for sampling map-plot residuals revealed that indeed $Pos(x)$ is small compared to the other error components. Omitting $Pos(x)$, the variance of difference between a map prediction AGB_{map} and reference AGB_{ref} at pixel x equals the sum of the remaining error variances (Equation 2):

$$Var(D(x)) = Var(M(x)) + Var(Plt(x)) + Var(S(x)) + Var(H(x)) \quad (2)$$

In our geostatistical modelling, we consider spatial correlation of $M(x)$, because errors in the AGB maps can be spatially correlated and we need to account for this in our model-based inference. We take into account this spatial correlation for purposes of assessing the joint AGB uncertainty when aggregating map data to larger support units, such as pixel blocks, countries or other regions of interest. Spatial correlation of $M(x)$ is modelled using biome-specific variograms, $\gamma_M(h)$ of *scaled* residuals, where h refers to a distance lag and –if necessary– the residuals are scaled by the standard deviations provided in the uncertainty layer accompanying the AGB map. Those (scaled) residuals are assumed second order stationary per biome.

We aim to model the bias $b(x)$ as a function of AGB_{map} and other spatially exhaustive covariates, as described in section 5.3.1.

	Ref	CCI Biomass Product Validation Plan v3		
	Issue	Page	Date	
	1.0	20	25-01-2021	

5.2. Identification of the error model

5.2.1. Overview



Table 2 provides an overview of the approaches for estimating the parameters of the uncertainty model described above. First results confirm an inverse relationship between $Var(Plt(x))$ and plot size, while $b(x)$ is often positive when the predicted AGB value is small (i.e., low AGB_{map} values tend to exceed AGB_{ref}) and negative when they are large (i.e., high AGB_{map} values in the map tend to be less than AGB_{ref}).

Table 2. Estimation methods for the parameters of the uncertainty model.

Component	Estimation approach
$b(x)$	Modelled as a function of AGB_{map} and spatially exhaustive covariates such as biome (Dinerstein et al. 2017), topographic variables and proxies for anthropogenic activity, using a random forest model (Breiman 2001) trained on observed differences, d_i , between AGB_{map} and AGB_{ref} data.
$Var(M(x))$	Square of the SD of the (zero mean) prediction error accompanying the CCI Biomass maps, as described in Quegan et al., (2017) and Santoro and Cartus (2019).
$Var(Plt(x))$	For a subset of plots having individual tree measurements, (Réjou-Méchain et al. 2017) biomass R-package is used. For other plots lacking such data, $Var(Plt(x))$ is predicted by a random forest model trained on the subset having individual tree measurements, using AGB_{map} , plot size and biomes as explanatory variables.
$Var(S(x))$	$Var(AGB^*_{pixel} - AGB^*_{plot}) = Var(AGB^*_{pixel}) + Var(AGB^*_{plot}) - 2 \cdot \sigma_{AGB^*_{pixel}, AGB^*_{plot}}$, where $\sigma_{AGB^*_{pixel}, AGB^*_{plot}}$ is the covariance of AGB^*_{pixel} and AGB^*_{plot} . All terms on the right-hand side of this equation are obtained from variograms of small, contiguously clustered sites within relevant Biomes, using change of support geostatistics (Goovaerts 1999, Malone et al. 2013). If nearby sites have different inventory dates, temporal adjustment to a common date is required, as described in section 3.4.
$Var(H(x))$	Variance of mathematical operations applied to random variables in the harmonization steps.
$\gamma_{AGB}(h)$	Variogram model fitted to experimental semivariances of AGB with a spatial support of the smallest plot size used. Used data are small-plot AGB_{plot} data, LiDAR -derived AGB or AGB_{plot} from larger plots, followed by deconvolution using a nugget-sill ratio borrowed from LiDAR data. Following Christensen (2011), the mean of $Var(Plt(x))$ is subtracted from the nugget.
$\gamma_M(h)$	Variogram model fitted to experimental semivariances of (scaled) residuals between AGB_{map} and AGB_{ref} after subtracting the bias $b(x)$. This variogram has a spatial support of map pixels. To correct for the other error sources, the mean variances $Var(Plt(x))$, $Var(S(x))$ and $Var(H(x))$ are subtracted from the nugget, following Christensen (2011). Scaling of the residuals may be needed to transform $M(x)$ to homoscedacity (see sections 5.1 and 5.2.3).

5.2.2. Variograms of AGB from small plots

As shown in Table 2, prediction of $Var(S(x))$ requires variograms of AGB from small, contiguously clustered sites located within relevant biomes ($\gamma_M(h)$). At the stage of writing, we have access to limited data from research plots and clustered NFI plots as well as LiDAR-derived AGB data from small footprints

	Ref	CCI Biomass Product Validation Plan v3		
	Issue	Page	Date	
	1.0	21	25-01-2021	

acquired over two forest sites in Remningstorp, Sweden, and Lope, Gabon, i.e., a *boreal* and a *tropical* forest site. The latter ALS datasets were acquired in the framework of the airborne ESA BIOSAR (Ulander et al., 2011). We still lack data for several biomes and expect these will be gathered in cooperation with WP1. Otherwise, we will apply variograms over broader geographical regions for which they are deemed appropriate.

Subplots from research plots are often larger (0.25ha) than the smallest plots of our dataset (a few plots are only 0.01ha). Variograms at the smallest support size will be obtained by variogram deconvolution (Goovaerts 2008) with a fixed nugget/sill ratio obtained from fine resolution AGB data, such as LiDAR-derived AGB. Following Christensen (2011), the mean variance of the plot measurement error is subtracted from the nugget variance.

5.2.3. Variograms of map error at the spatial support of map pixels

Spatial aggregation of uncertainty over larger support units (see section 5.3.4) requires variograms of $M(\cdot)$ at pixel support ($\gamma_M(h)$). The uncertainty layer of the CCI Biomass maps and the other uncertainties considered in section 5.1 acknowledge that we expect $Var(D(x))$ to vary over space (i.e., it is heteroscedastic). In other words, we recognize that at some locations, larger deviations between AGB_{map} and AGB_{ref} are more likely to occur than at other locations. If necessary, observed realizations of $D(x) - b(x)$ are scaled by $\sqrt{Var(M(x))}$ aiming to achieve homoscedasticity. Again, the (Christensen 2011) approach for heterogeneous measurement error variances will be used for estimating the variogram of the unobserved $M(\cdot)$ at pixel support, using estimated values for each error component as listed in Table 2.

5.3. Model-based prediction



5.3.1. Bias trend prediction

Different forest types, climatic gradients, topography and AGB itself have been found to affect bias in biomass predictions (Chave et al. 2004, Rodríguez-Veiga et al. 2019, Santoro et al. 2015). We try to model this bias as a function of AGB_{map} and its textural properties as well as other spatially exhaustive covariates such as biome (Dinerstein et al. 2017), topographic variables (elevation, slope), canopy height and a proxy for anthropogenic activity (population density) using a random forest model (Breiman 2001). The approach is documented in more detail in Araza et al. (forthcoming).

The predictive power of the covariates is evaluated using variable importance measures while sensitivity of the modelled trends to its inputs is assessed using partial dependence plots (Greenwell 2017). If fitting the bias trend model is successful, the random forest model is used in predictive mode to predict a global bias layer $b(x)$. Statistical significance of predicted bias is assessed using the prediction standard errors obtained with Wager's et al. (2014) infinitesimal jack-knife approach.

5.3.2. Error budgeting

The error model presented in section 5.1 allows comparison of $Var(D(x))$ observed over AGB_{ref} bins with the sum of the error variances at the right-hand side of Equation (2). In de Bruin et al. (2019b, 2020b), a similar partial comparison was used to assess whether the uncertainty layer provided with the

	Ref	CCI Biomass Product Validation Plan v3		
	Issue	Page	Date	
	1.0	22	25-01-2021	

CCI Biomass map is consistent with considered error variances. This comparison can only be completed if the error model has been fully identified (section 5.2).

5.3.3. Block kriging for map-plot comparison at supra pixel support

Section 4.3.1 referred to a third option for computing the mean temporally adjusted AGB_{ref} at the spatial support of 0.1° cells by block kriging. This is achieved by computing block averages of AGB from within-block and nearby temporally adjusted plot AGB using the small plot variograms introduced in section 5.2.2 and block kriging that accounts for different error variances of the plot data (Malone et al. 2013). The procedure also computes the variance of the prediction error. Correcting for forest fraction (section 3.4), AGB_{ref} at 0.1° cell level is obtained, which is compared with the average AGB_{map} over the 0.1° cell. It is repeated here that this procedure is only possible if variograms of AGB at the spatial support of the smallest plots are available for the different forest types.

5.3.4. Spatial aggregation of random error

Spatially uncorrelated zero-mean errors tend to cancel out when aggregating over larger spatial units, but this effect is less pronounced when errors are spatially correlated. We model the latter effect using the variograms introduced in section 5.2.3. From the variograms and the distance matrix for all pixel pairs, x_i, x_j contained in a support unit, a covariance matrix, Σ , is computed with elements $\sigma_{i,j}$. The variance of the map error over the support unit is then predicted by summing the elements of Σ and division by n^2 (Equation 3):

$$Var(agr) = \frac{1}{n^2} \sum_{i=1}^n \sum_{j=1}^n \sigma_{i,j} \quad (3)$$

6. Map inter-comparison

6.1. Stability of $AGB_{map} - AGB_{ref}$ among CCI Biomass products

According to the World Meteorological Organization (2011), stability is the extent to which the error of a product remains constant over a long period of time. To explore local stability of plot-map differences (d_i) over the three AGB epochs produced within the CCI Biomass project, we suggest to produce scatterplots of d_i for each combination of map reference years, as exemplified in Figure 6.

The map producer may want to know *where* the largest instabilities in the residuals occur. Such information can be provided by plotting the locations of chosen tails of the distribution of differences in d_i for different combinations of reference years (e.g., the 5% sites with the most negative differences and the sites of the 5% largest positive differences). Alternatively, sites where the instability exceeds a particular threshold (e.g., 10%, as proposed by the World Meteorological Organization²) can be of interest.

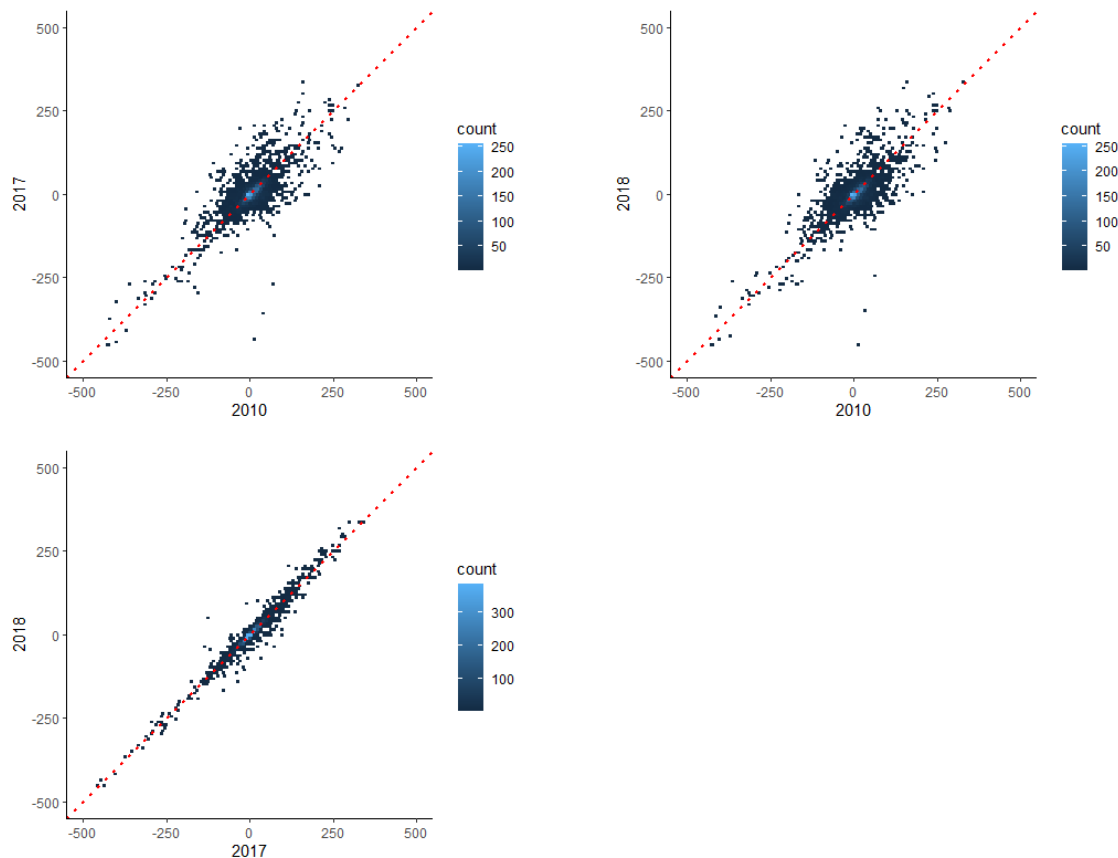




Figure 5. AGB residuals between harmonized tier1-3 plot data and mapped AGB at 0.1° cell level for each combination of map reference years. The red dashed line is the 1:1 line.

² <https://gcos.wmo.int/en/essential-climate-variables/biomass/ecv-requirements>

	Ref	CCI Biomass Product Validation Plan v3		
	Issue	Page	Date	
	1.0	24	25-01-2021	

6.2. Comparison of CCI Biomass maps with other AGB products

This task consists of the comparison of the CCI Biomass maps with other AGB products covering a given geographic extent, as well as comparison of map bias based on AGB reference data. The comparison aims to complement product validation with the following information: evaluation of consistency between different products; identification of areas with larger disagreements and assessment of whether these areas need further study; assessment of strengths and weaknesses of different datasets based on the analysis of the data and methods used to produce the maps; and increased awareness and acceptance of CCI Biomass products within the international community.

The map inter-comparison involves the following steps. Firstly, datasets to be compared (i.e., regional or global maps) are identified and acquired. Secondly, the datasets are harmonized with CCI Biomass maps in terms of spatial and temporal support (see section 3.4) as well as thematic content (e.g., biomass unit). Thirdly, the following comparison metrics are computed at pixel level and at aggregated grid resolution (e.g., 0.1°):

1. Comparison statistics, global and over continents and ecological zones:
 - Mean (absolute) difference
 - Histogram of differences
 - Root Mean Square Difference
 - Linear correlation
2. Comparison maps:
 - Difference maps
 - Relative difference maps, using the CCI Biomass maps as reference
3. Comparison plots of mapped data:
 - Scatterplots or whisker plots such as exemplified in Figure 6.
 - Histograms and cumulative distributions
4. Comparison plots of mapped data against harmonized AGB plot data, such as exemplified in Figure 6.

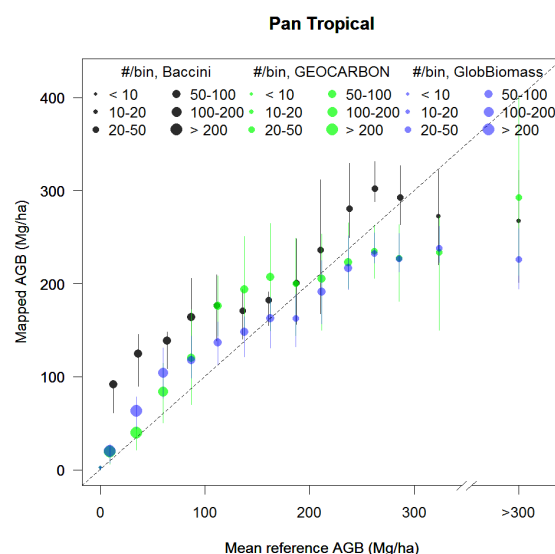


Figure 6. Example comparison of different global biomass maps (Baccini, GOCARBON and GlobBiomass) against harmonized plot data.

7. Expert assessment

The Expert Assessment is an essential quality control and feedback mechanism, aimed at assessing the users' acceptance of CCI Biomass products, evaluating their quality and limitations from the users' perspective, and obtaining recommendations for improvements. The output of the user assessment consists of an Expert Survey report.

The user assessment is performed using standard questionnaires, which are produced for each CCI Biomass product and will be sent to users within and beyond the project consortium. The questionnaires aim to assess:

- User satisfaction
- Product usability
- Delivery system (timing, delivery method, naming, format, etc.)
- Product quality and limitations related to spatial and temporal resolution
- Applicability of the products for climate modelling
- Need of capacity building (optional)
- Future data and product requirements

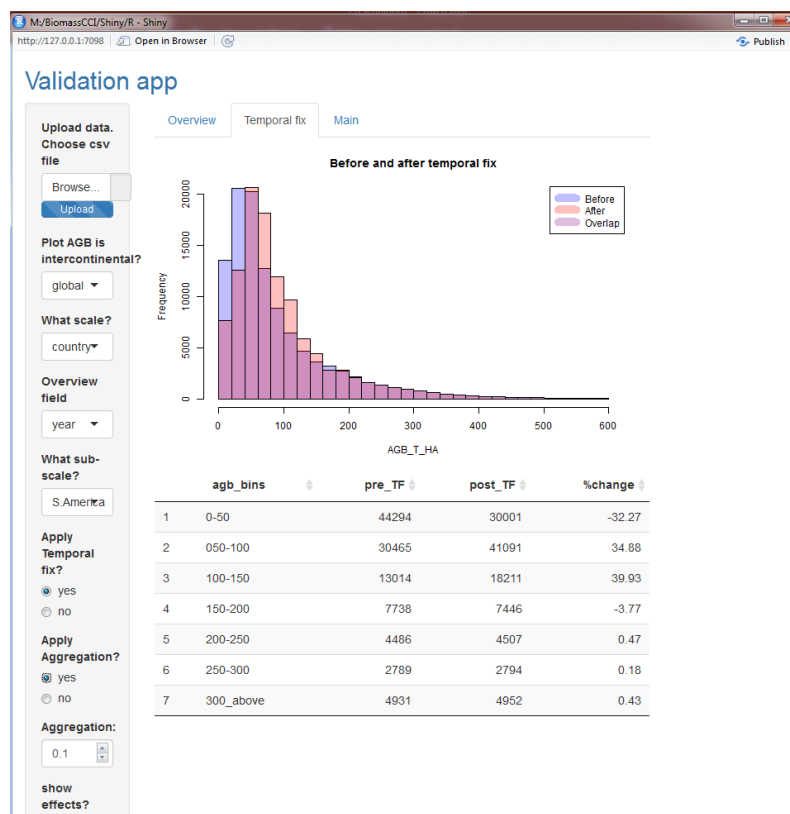




Figure 7. Screenshot of a prototype analysis tool provided with the R package for expert assessment.



To support users in assessing the CCI Biomass products using their own data, an R-workflow is being implemented in tools intended for distinct user groups: (1) an online interactive tool for occasional

	Ref	CCI Biomass Product Validation Plan v3		
	Issue	Page	Date	
	1.0	26	25-01-2021	

users, which provides easy access to the analysis methods described in this validation plan, and (2) an offline toolbox for technical users who want to integrate the analysis methods in their own workflow, i.e., third parties who conduct independent validation. Figure 7 shows a screenshot of a prototype the online interactive tool; the local version can be found at:



https://github.com/arnanaraza/PlotToMap_Local. The local version has been tested by users from the University of Leicester, Forest Research and the World Resources Institute.

The main functionalities of the R workflow include pre-processing of different forest inventory configurations (e.g., plot shapes), estimation of measurement error for plot data with and without tree-level measurement and visualization of plot-to-map comparisons.



	Ref	CCI Biomass Product Validation Plan v3		
	Issue	Page	Date	
	1.0	27	25-01-2021	

References

- Avitabile, V., Balzter, H., de Bruin, S., Carreiras, J., Carvalhais, N., Quegan, S., Tansey, K. and Rodriguez-Veiga, P. (2015) DUE GlobBiomass - Validation Protocol, Wageningen University and Research Centre.
- Araza, A., et al., Comparing aboveground biomass from plots and global maps: Towards a comprehensive uncertainty assessment (Forthcoming).
- Breiman, L. (2001) Random Forests. *Machine Learning* 45(1), 5-32.
- Chave, J., Condit, R., Aguilar, S., Hernandez, A., Lao, S. and Perez, R. (2004) Error propagation and scaling for tropical forest biomass estimates. *Philosophical transactions of the Royal Society of London. Series B, Biological sciences* 359(1443), 409-420.
- Christensen, W.F. (2011) Filtered Kriging for Spatial Data with Heterogeneous Measurement Error Variances. *Biometrics* 67(3), 947-957.
- de Bruin, S., Herold, M. and Araza, A. (2019a) CCI Biomass Product Validation Plan, Year 1, Version 1.
- de Bruin, S., Herold, M., Araza, A., Kay, H. and Lucas, R. (2019b) Product validation & intercomparison report, year 1, version 1.1.
- de Bruin, S., Herold, M. and Araza, A. (2020a) CCI Biomass Product Validation Plan, Year 2, Version 2.
- de Bruin, S., Herold, M., Araza, A., Kay, H. and Lucas, R. (2020b) Product validation & intercomparison report, year 2, version 2.
- Dinerstein, E., Olson, D., Joshi, A., Vynne, C., Burgess, N.D., Wikramanayake, E., Hahn, N., Palminteri, S., Hedao, P., Noss, R., Hansen, M., Locke, H., Ellis, E.C., Jones, B., Barber, C.V., Hayes, R., Kormos, C., Martin, V., Crist, E., Sechrest, W., Price, L., Baillie, J.E.M., Weeden, D., Suckling, K., Davis, C., Sizer, N., Moore, R., Thau, D., Birch, T., Potapov, P., Turubanova, S., Tyukavina, A., de Souza, N., Pintea, L., Brito, J.C., Llewellyn, O.A., Miller, A.G., Patzelt, A., Ghazanfar, S.A., Timberlake, J., Klöser, H., Shennan-Farpón, Y., Kindt, R., Lillesø, J.-P.B., van Breugel, P., Graudal, L., Vogé, M., Al-Shammari, K.F. and Saleem, M. (2017) An Ecoregion-Based Approach to Protecting Half the Terrestrial Realm. *BioScience* 67(6), 534-545.
- Goovaerts, P. (1999) Geostatistical Tools for Deriving Block-Averaged Values of Environmental Attributes. *Geographic Information Sciences* 5(2), 88-96.
- Goovaerts, P. (2008) Kriging and Semivariogram Deconvolution in the Presence of Irregular Geographical Units. *Mathematical Geosciences* 40(1), 101-128.
- Greenwell, B.M. (2017) pdp: An R package for constructing partial dependence plots. *R Journal* 9(1), 421-436.
- Hansen, M.C., Potapov, P.V., Moore, R., Hancher, M., Turubanova, S.A., Tyukavina, A., Thau, D., Stehman, S.V., Goetz, S.J., Loveland, T.R., Kommareddy, A., Egorov, A., Chini, L., Justice, C.O. and Townshend, J.R.G. (2013) High-Resolution Global Maps of 21st-Century Forest Cover Change. *Science* 342(6160), 850-853.
- Hijmans, R.J. (2017) raster: Geographic Data Analysis and Modeling.
- Horn, B. (1981) Hill shading and the reflectance map. *Proceedings of the IEEE* 69, 14-47.
- Labrière, N., Tao, S., Chave, J., Scipal, K., Toan, T.L., Abernethy, K., Alonso, A., Barbier, N., Bissiengou, P., Casal, T., Davies, S.J., Ferraz, A., Hérault, B., Jaouen, G., Jeffery, K.J., Kenfack, D., Korte, L., Lewis, S.L., Malhi, Y., Memiaghe, H.R., Poulsen, J.R., Réjou-Méchain, M., Villard, L., Vincent, G., White, L.J.T. and Saatchi, S. (2018) In Situ Reference Datasets From the TropiSAR and AfriSAR Campaigns in Support of Upcoming Spaceborne Biomass Missions. *IEEE Journal of Selected Topics in Applied Earth Observations and Remote Sensing* 11(10), 3617-3627.
- Labrière, N., & Chave, J. (2020a) CCI Biomass project – In situ datasets: Processing and validation of Sustainable Landscape Brazil data (CCI Biomass internal report).
- Labrière, N., & Chave, J. (2020b) CCI Biomass project – In situ datasets: Processing and validation of NEON data (USA) (CCI Biomass internal report).
- Labrière, N., & Chave, J. (2020c) In situ datasets: Processing and validation of TERN data (CCI Biomass internal report).
- Lucas, R., Butting, P., Kay, H. and Santoro, M. (2020) Data access requirements document year 3 version 2.0.
- Malone, B.P., McBratney, A.B. and Minasny, B. (2013) Spatial scaling for digital soil mapping. *Soil Science Society of America Journal* 77(3), 890-902.
- Olofsson, P., Foody, G.M., Herold, M., Stehman, S.V., Woodcock, C.E. and Wulder, M.A. (2014) Good practices for estimating area and assessing accuracy of land change. *Remote Sensing of Environment* 148, 42-57.



	Ref	CCI Biomass Product Validation Plan v3		
	Issue	Page	Date	
	1.0	28	25-01-2021	

- Ploton, P., Mortier, F., Barbier, N. et al. (2020). A map of African humid tropical forest aboveground biomass derived from management inventories. *Sci Data* 7, 221.
- Quegan, S. and Ciais, P. (2018) CCI BIOMASS User Requirement Document Year 1
- Réjou-Méchain, M., Barbier, N., Coutron, P., Ploton, P., Vincent, G., Herold, M., Mermoz, S., Saatchi, S., Chave, J., de Boissieu, F., Féret, J.-B., Takoudjou, S.M. and Pélissier, R. (2019) Upscaling Forest Biomass from Field to Satellite Measurements: Sources of Errors and Ways to Reduce Them. *Surveys in Geophysics*.
- Réjou-Méchain, M., Muller-Landau, H.C., Detto, M., Thomas, S.C., Le Toan, T., Saatchi, S.S., Barreto-Silva, J.S., Bourg, N.A., Bunyavejchewin, S., Butt, N., Brockelman, W.Y., Cao, M., Cárdenas, D., Chiang, J.M., Chuyong, G.B., Clay, K., Condit, R., Dattaraja, H.S., Davies, S.J., Duque, A., Esufali, S., Ewango, C., Fernando, R.H.S., Fletcher, C.D., N. Gunatilleke, I.A.U., Hao, Z., Harms, K.E., Hart, T.B., Hérault, B., Howe, R.W., Hubbell, S.P., Johnson, D.J., Kenfack, D., Larson, A.J., Lin, L., Lin, Y., Lutz, J.A., Makana, J.R., Malhi, Y., Marthens, T.R., McEwan, R.W., McMahon, S.M., McShea, W.J., Muscarella, R., Nathalang, A., Noor, N.S.M., Nytch, C.J., Oliveira, A.A., Phillips, R.P., Pongpattananurak, N., PUNCHI-Manage, R., Salim, R., Schurman, J., Sukumar, R., Suresh, H.S., Suwanvecho, U., Thomas, D.W., Thompson, J., Uriarte, M., Valencia, R., Vicentini, A., Wolf, A.T., Yap, S., Yuan, Z., Zartman, C.E., Zimmerman, J.K. and Chave, J. (2014) Local spatial structure of forest biomass and its consequences for remote sensing of carbon stocks. *Biogeosciences* 11(23), 6827-6840.
- Réjou-Méchain, M., Tanguy, A., Piponiot, C., Chave, J. and Hérault, B. (2017) biomass: an r package for estimating above-ground biomass and its uncertainty in tropical forests. *Methods in Ecology and Evolution* 8(9), 1163-1167.
- Rodríguez-Veiga, P., Quegan, S., Carreiras, J., Persson, H.J., Fransson, J.E.S., Hoscilo, A., Ziótkowski, D., Stereńczak, K., Lohberger, S., Stängel, M., Berninger, A., Siegert, F., Avitabile, V., Herold, M., Mermoz, S., Bouvet, A., Le Toan, T., Carvalhais, N., Santoro, M., Cartus, O., Rauste, Y., Mathieu, R., Asner, G.P., Thiel, C., Pathe, C., Schmullius, C., Seifert, F.M., Tansey, K. and Balzter, H. (2019) Forest biomass retrieval approaches from earth observation in different biomes. *International Journal of Applied Earth Observation and Geoinformation* 77, 53-68.
- Rozendaal, D.M.A., Santoro, M., Schepaschenko, D., Avitabile, V. and Herold, M. (2017) DUE GlobBiomass D17 Validation Report, p. 26, European Space Agency (ESA-ESRIN).
- Santoro, M., Eriksson, L.E.B. and Fransson, J.E.S. (2015) Reviewing ALOS PALSAR backscatter observations for stem volume retrieval in Swedish forest. *Remote Sensing* 7(4), 4290-4317.
- Ulander, L.M.H., Gustavsson, A., Flood, B., Murdin, D., Dubois-Fernandez, P., Dupuis, X., Sandberg, G., Soja, M.J., Eriksson, L.E.B., Fransson, J.E.S., Holmgren, J., Wallerman, J. (2011). BioSAR 2010 - Technical assistance for the development of airborne SAR and geophysical measurements during the BioSAR 2010 experiment.
- Wager, S., Hastie, T. and Efron, B. (2014) Confidence intervals for random forests: The jackknife and the infinitesimal jackknife. *Journal of Machine Learning Research* 15, 1625-1651.
- World Meteorological Organization (2011). Systematic observation requirements for satellite-based data products for climate: Supplemental details to the satellite-based component of the Implementation Plan for the Global Observing System for Climate in Support of the UNFCCC (2010 Update). https://library.wmo.int/doc_num.php?explnum_id=3710.



	Ref	CCI Biomass Product Validation Plan v3		
	Issue	Page	Date	
	1.0	29	25-01-2021	

APPENDIX 1. Plot data used for validating CCI Biomass products.



ID	Tier	Average year	Average size (ha)	Count	Biome	URL	Paper/ source	Data access
AFR_L	3	2011	25.00	1	Tropical rainforest	https://dspace.stir.ac.uk/retrieve/74d3b352-fa46-418f-ba95-728bb33f4fc/08417912.pdf	(Labrière et al., 2018)	open
EU_FOS	3	2014	16.25	1	Tropical rainforest	https://www.-ture.com/articles/s41597-019-0196-1?fbclid=IwAR08vLoOm4xEQo4EUdLtoKsnP6nsNIY5CYnfcoqGcS5Z0_UcyaNlr-jcdDg	(Schepaschenko et al., 2019)	open
SAM_L	3	2010	7.65	20	Tropical rainforest	https://dspace.stir.ac.uk/retrieve/74d3b352-fa46-418f-ba95-728bb33f4fc/08417912.pdf	(Labrière et al., 2018)	open
AUS1	3	2009	25.00	1	Tropical dry forest	http://data.auscover.org.au/xwiki/bin/view/Product+pages/Biomass+Plot+Library	(Paul et al., 2016)	source-WUR agreement
SAM_RF	3	2008	5.3	10	Tropical rainforest	http://www.rainfor.org/en/project/about-rainfor	Lopez-Gonzales et al., 2011	Open
AFR_FOS	2	2013	1.00	44	Tropical rainforest	https://www.-ture.com/articles/s41597-019-0196-1?fbclid=IwAR08vLoOm4xEQo4EUdLtoKsnP6nsNIY5CYnfcoqGcS5Z0_UcyaNlr-jcdDg	(Schepaschenko et al., 2019)	open
AFR_L	2	2016	1.00	56	Tropical rainforest	https://dspace.stir.ac.uk/retrieve/74d3b352-fa46-418f-ba95-728bb33f4fc/08417912.pdf	(Labrière et al., 2018)	open
AUS_FOS	2	2008	1.00	2	Tropical dry forest	https://www.-ture.com/articles/s41597-019-0196-1?fbclid=IwAR08vLoOm4xEQo4EUdLtoKsnP6nsNIY5CYnfcoqGcS5Z0_UcyaNlr-jcdDg	(Schepaschenko et al., 2019)	open
CAM_FOS	2	2012	1.01	18	Tropical rainforest	https://www.-ture.com/articles/s41597-019-0196-1?fbclid=IwAR08vLoOm4xEQo4EUdLtoKsnP6nsNIY5CYnfcoqGcS5Z0_UcyaNlr-jcdDg	(Schepaschenko et al., 2019)	open
EU_FOS	2	2010	2.23	2	Boreal coniferous forest	https://www.-ture.com/articles/s41597-019-0196-1?fbclid=IwAR08vLoOm4xEQo4EUdLtoKsnP6nsNIY5CYnfcoqGcS5Z0_UcyaNlr-jcdDg	(Schepaschenko et al., 2019)	open
SAM_FOS	2	2011	1.00	23	Tropical rainforest	https://www.-ture.com/articles/s41597-019-0196-1?fbclid=IwAR08vLoOm4xEQo4EUdLtoKsnP6nsNIY5CYnfcoqGcS5Z0_UcyaNlr-jcdDg	(Schepaschenko et al., 2019)	open
SAM_L	2	2013	1.04	28	Tropical rainforest	https://dspace.stir.ac.uk/retrieve/74d3b352-fa46-418f-ba95-728bb33f4fc/08417912.pdf	(Labrière et al., 2018)	open
SAM_BAJ	2	2017	1	3	Tropical rainforest	https://ieeexplore.ieee.org/abstract/document/8518871	Pacheco-Pascagaza et al., 2020	source-WUR agreement
SAM_RF	2	2008	1	374	Tropical rainforest	http://www.rainfor.org/en/project/about-rainfor	Lopez-Gonzales et al., 2011	Open

	Ref	CCI Biomass Product Validation Plan v3			
	Issue	Page	Date		
	1.0	30	25-01-2021		

UK_FOS	2	2015	1.20	1	Tropical rainforest	https://www.-ture.com/articles/s41597-019-0196-1?fbclid=IwAR08vLoOm4xEQo4EUdLtoKsnP6nsNIY5CYnfcqGcS5Z0_UcyaNlr-jcdDg	(Schepaschenko et al., 2019)	open
AFR10	2	2007	1.00	7	Tropical rainforest	https://iopscience.iop.org/article/10.1088/1748-9326/6/4/049001/meta	(Mitchard et al., 2011)	source-WUR agreement
AFR13	2	2008	1.00	2	Tropical rainforest	https://agupubs.onlinelibrary.wiley.com/doi/full/10.1029/2009GL040692	(Mitchard et al., 2009)	source-WUR agreement
AFR14	2	2009	1.63	4	Tropical rainforest	https://www.sciencedirect.com/science/article/abs/pii/S014362281400109X	(Ryan, Berry, & Joshi, 2014)	source-WUR agreement
AFR6	2	2009	1.00	12	Tropical rainforest	https://cbmjour-l.biomedcentral.com/articles/10.1186/1750-0680-9-2	(Willcock et al., 2014)	source-WUR agreement
AFR7	2	2012	1.00	19	Tropical rainforest	https://royalsocietypublishing.org/doi/full/10.1098/rstb.2012.0295	(Lewis et al., 2013)	source-WUR agreement
ASI3	2	2007	1.00	92	Tropical rainforest	https://www.sciencedirect.com/science/article/abs/pii/S0378112711004361	(Morel et al., 2011)	source-WUR agreement
AUS1	2	2012	1.01	63	Subtropical steppe	http://data.auscover.org.au/xwiki/bin/view/Product+pages/Biomass+Plot+Library	(Paul et al., 2016)	source-WUR agreement
SAM2	2	2012	1.00	40	Tropical rainforest	http://geoinfo.cnpm.embrapa.br/geonetwork/srv/eng/main.home		source-WUR agreement
SAM_FOS	1	2011	0.25	142	Tropical rainforest	https://www.-ture.com/articles/s41597-019-0196-1?fbclid=IwAR08vLoOm4xEQo4EUdLtoKsnP6nsNIY5CYnfcqGcS5Z0_UcyaNlr-jcdDg	(Schepaschenko et al., 2019)	open
AFR15	1	2013	0.25	136	Tropical rainforest	https://besjour-ls.onlinelibrary.wiley.com/doi/full/10.1111/1365-2745.12548%4010.1111/%28ISSN%291365-2745.FORESTRY	(Vieilledent et al., 2016)	source-WUR agreement
AFR1	1	2008	0.50	1152	Tropical rainforest	https://agritrop.cirad.fr/572060/1/document_572060.pdf	(Hirsh, Jourget, Feintrenie, Bayol, & Ebaá Atyi, 2013)	source-WUR agreement
AFR10	1	2007	0.50	11	Tropical rainforest	https://iopscience.iop.org/article/10.1088/1748-9326/6/4/049001/meta	(Mitchard et al., 2011)	source-WUR agreement
AFR12	1	2008	0.16	108	Tropical rainforest	https://www.sciencedirect.com/science/article/abs/pii/S0034425711003609	(Avitabile, Baccini, Friedl, & Schmullius, 2012)	source-WUR agreement
AFR13	1	2008	0.50	23	Tropical rainforest	https://agupubs.onlinelibrary.wiley.com/doi/full/10.1029/2009GL040692	(Mitchard et al., 2009)	source-WUR agreement
AFR14	1	2009	0.51	70	Tropical dry forest	https://www.sciencedirect.com/science/article/abs/pii/S014362281400109X	(Ryan et al., 2014)	source-WUR agreement
AFR4	1	2012	0.13	110	Tropical mountain system	http://www.geo-informatie.nl/workshops/scw2/papers/deVries.pdf	(DeVries, Avitabile, Kooistra, & Herold, 2012)	source-WUR agreement

	Ref	CCI Biomass Product Validation Plan v3			
	Issue	Page	Date		
	1.0	31	25-01-2021		

AFR5	1	2012	0.08	71	Tropical rainforest	https://pure.mpg.de/pubman/faces/ViewItemOverviewPage.jsp?itemId=item_2281402	(Vaglio Laurin et al., 2016)	source-WUR agreement
AFR6	1	2009	0.33	12	Tropical dry forest	https://cbmjour-l.biomedcentral.com/articles/10.1186/1750-0680-9-2	(Willcock et al., 2014)	source-WUR agreement
AFR8	1	2008	0.13	105	Tropical moist forest	https://www.sciencedirect.com/science/article/abs/pii/S0034425712001058	(Carreiras, Vasconcelos, & Lucas, 2012)	source-WUR agreement
AFR9	1	2016	0.13	9642	Tropical dry forest	https://www.mdpi.com/2072-4292/5/4/1524 https://fndsmoz.maps.arcgis.com/apps/MapSeries/index.html?appid=6602939f39ad4626a10f87bf6253af1e	(Carreiras et al., 2012)	open, source-WUR agreement
AFR_KEN	1	2011	0.09	362	Tropical and subtropical grasslands, savannas and shrublands			source-WUR agreement
ASI1	1	2008	0.05	2903	Tropical mountain system and rainforest	https://www.tandfonline.com/doi/full/10.1080/17583004.2016.1254009	(Avitabile et al., 2016)	source-WUR agreement
ASI10	1	2008	0.10	1268	Subtropical mountain system	https://www.sciencedirect.com/science/article/abs/pii/S0034425719303608	Zhang et al. 2019	source-WUR agreement
ASI2	1	2011	0.11	119	Tropical dry forest	http://www.leafasia.org/sites/default/files/public/resources/WWF-REDD-pres-July-2013-v3.pdf	WWF and OBF, 2013	source-WUR agreement
ASI4	1	2010	0.02	70	Tropical dry forest	http://citeseerx.ist.psu.edu/viewdoc/download?doi=10.1.1.972.708&rep=rep1&type=pdf	Wijaya et al., 2015	source-WUR agreement
ASI9	1	2012	0.13	74	Tropical rainforest	http://leutra.geogr.uni-je.-de/vgtbRBIS/metadata/start.php	Avitabile et al., 2014	source-WUR agreement
ASI_FOS	1	2014	0.25	2	Tropical rainforest	https://www.-ture.com/articles/s41597-019-0196-1?fbclid=IwAR08vLoOm4xEQo4EUdLtoKsnP6nsNIY5CYnfcogGcS5Z0_UcyaNlr-jcdDg	(Schepaschenko et al., 2019)	open
AUS1	1	2011	0.12	5611	Tropical dry forest	http://data.auscover.org.au/xwiki/bin/view/Product+pages/Biomass+Plot+Library	Paul et al. 2016	source-WUR agreement
EU1	1	2011	0.01	16819	Temperate broadleaf and mixed forests and Boreal forests	https://www.slu.se/en/collaborative-centres-and-projects/swedish--tio-l-forest-inventory/	Sweden NFI	source-WUR agreement
EU2	1	2007	0.20	7177	Mediterranean forests	http://www.magrama.gob.es/es/desarrollo-rural/temas/politica-forestal/inventario-cartografia/inventario-forestal--cio-l/	Spain NFI	source-WUR agreement
EU3	1	2013	0.06	3021	Temperate oceanic forest	https://library.wur.nl/WebQuery/wurpubs/454875	Netherlands NFI	source-WUR agreement

	Ref	CCI Biomass Product Validation Plan v3			
	Issue	Page	Date		
	1.0	32	25-01-2021		

EU4	1	2007	0.06	5967	Temperate broadleaf and mixed forests and Mediterranean forests	https://www.agriculturejour-ls.cz/publicFiles/01003.pdf	Cienciela et al. 2008	source-WUR agreement
EU_FOS	1	2015	0.28	514	Boreal forests	https://www.-ture.com/articles/s41597-019-0196-1?fbclid=IwAR08vLoOm4xEQo4EUdLtoKsnP6nsNIY5CYnfcqGcS5Z0_UcyaNlr-jcdDg	(Schepaschenko et al., 2019)	open, source-WUR agreement
NAM1	1	2010	0.04	586	Boreal coniferous forest	https://www.p-s.org/content/112/18/5738.short	Liang et al., 2015	source-WUR agreement
NAM2	1	2004	0.04	75	Temperate mountain system	https://www.nature.com/articles/nature07276	Luyssaert et al., 2008	source-WUR agreement
NAM3	1	2010	0.03	588	Temperate continental forest			source-WUR agreement
NAM4	1	2010	0.04	2794	Temperate mountain system		Alaska NFI	source-WUR agreement
SAM2	1	2013	0.23	241	Tropical rainforest	https://www.paisagenslidar.cnptia.embrapa.br/webgis/	Embrapa, undated	source-WUR agreement
SAM3	1	2011	0.13	111	Tropical rainforest		CIFOR, undated	source-WUR agreement
SAM4	1	2014	0.15	7	Tropical rainforest		CIFOR, undated	source-WUR agreement
SAM5	1	2014	0.60	23	Tropical rainforest		CIFOR, undated	source-WUR agreement
SAM_BAJ	1	2017	0.25	363	Tropical rainforest	https://ieeexplore.ieee.org/abstract/document/8518871	Pacheco-Pascagaza et al., 2020	source-WUR agreement
SAM_RF	1	2008	1	125	Tropical rainforest	http://www.rainfor.org/en/project/about-rainfor	Lopez-Gonzales et al., 2011	Open
SAM_TAP A	1	2009	0.5	138	Tropical rainforest	https://www.tandfonline.com/doi/full/10.1080/07038992.2014.913477?casa_token=EZxeZoegekKAAAAA%3AZHCN98XtpZRrsS9KogTBhPy1_yzhAkkLZHfck3fomwSnvSaO7YDiuP_V_hne6Mj1Wdn-7ME_sPChP	(Bispo et al., 2014)	source-WUR agreement
AFR_COF	0	2009	100	35029	Tropical moist forest,	https://www.nature.com/articles/s41597-020-0561-0	(Ploton et al., 2020)	open
LIDAR	0	2014	1	744397	Tropical rainforest		SLB, TERN, NEON	open